IET Generation, Transmission & Distribution

Research Article

Start-up and recovery method with LCC–HVDC systems participation during AC/DC system black-starts

ISSN 1751-8687
Received on 28th June 2018
Revised 17th June 2019
Accepted on 3rd September 2019
E-First on 10th December 2019
doi: 10.1049/iet-gtd.2018.6042
www.ietdl.org

Xinwei Li[1], *Chongru Liu*[1] ✉, *YuanYuan Lou*[2]
[1]*North China Electric Power University, No. 2 Beinong Road, Beijing, People's Republic of China*
[2]*Power Dispatching Control Center of Guangdong Power Grid Co., Ltd, Guangdong, People's Republic of China*
✉ *E-mail: chongru.liu@ncepu.edu.cn*

Abstract: With the increase in a number of online high-voltage direct current (HVDC) systems in China, a big question for their use as black-start and restoration of power system outages arises. Line-commutated converters (LCC)–HVDC systems can significantly reduce recovery time. The black-start-up and recovery conditions for LCC–HVDC systems and the connected AC systems are discussed in this study. The appropriate start-up and recovery modes are identified and the results of the control characteristics of LCC–HVDC systems are analysed in detail. The stability requirements of AC systems in terms of LCC–HVDC system effects are evaluated. Furthermore, the restoration using LCC–HVDC systems, including the priority sequence index of the multi-HVDC links and the optimisation model of the mentioned problem, is discussed in detail. Compared to the conventional black-start strategy, the applicability and effectiveness of the proposed method are illustrated using a part of the actual Guangzhou power system as a test system.

1 Introduction

With the development of power networks, the interconnection of power grids through line-commutated converters (LCC)–high-voltage direct current (HVDC) transmission lines becomes necessary, especially in China. This increases security risks, such as recent major blackouts including the blackout in Australia on 28 September 2016, and the power outage in India on 30 July 2012 [1–3]. The aim of post-blackout restoration is to ensure the quick restoration and safe operation of the system [4]. To date, most research and applications are focused on power system restoration of the AC grid. In-depth analyses have explored the selection of the black-start power source, the black-start path, load recovery, and security verification [5–8]. Current black-start modes use self-starting generators and self-priming hydropower units as power sources, following by gradual online return of large conventional power plants. However, such conventional restoration is slow and produces large spikes as auxiliary engines fire up, compromising load recovery. An optimised two-step start strategy was proposed in [9]; the generator recovery sequence was obtained using the maximum generator capacity as the objective function. The recovery path was optimised by reference to the relative importance of buses and the synchronisation recovery mode.

HVDC systems are highly controllable, afford rapid start-up & adjustment and permit transmission of bulk amount of power. Today a bulk number of HVDC links have been constructed. However, conventional black-start models do not involve LCC–HVDC systems. The reasons come from two aspects: (i) power grids in the early stage of black-start is vulnerable, which strength is generally considered as ‘weak’ relative to the capacity of the DC link [10]; (ii) research on the practical control of LCC–HVDC systems used for black-start and restoration is insufficient. The question arises: how can LCC–HVDC systems be used to enhance restoration and start-up speed? The conditions that are necessary to start an LCC–HVDC system, the black-start path, and the methods of a start-up are roughly discussed in [11], considering the ±500 kV Tian-Guang and ±800 kV Yun-Guang HVDC systems. The rare paper discusses the start-up and recovery method of LCC–HVDC transmission system in black-start. Considering the feathers of LCC–HVDC systems, the following problems should be answered: (i) the cooperation between LCC–HVDC system and power plants when restarting; (ii) the necessary requirements for the AC and LCC–HVDC systems to reduce start-up time as well as keep stable.

To solve these problems, a start-up and recovery method with LCC–HVDC systems participation during AC/DC system black-starts is presented in this study to explore whether HVDC systems can be used for black-starting reliably or not. The start-up and recovery of systems featuring both LCC–HVDC systems and conventional power plants are considered. Section 2 discusses control methods for LCC–HVDC systems during start-up and recovery. In Section 3 the details of the features required by HVDC-linked AC systems participating in black-start are discussed. Section 4 is a detailed analysis and calculation method of a black-start involving LCC–HVDC systems. Section 5 proves the utility of the proposed method and Section 6 draws conclusions. In this study, HVDC systems refer to LCC–HVDC systems.

2 Requirements for HVDC start-up and restoration

2.1 HVDC start-up mode

As the AC systems connected HVDC links are weak during restoration, it is important to guarantee voltage stability of the joint bus, so the stable bus can help to keep the HVDC system operating normally during black-start [12]. Several control modes are available during the process of black-start: (i) the constant power (CP) at rectifier and constant extinction angle (CEA) at inverter control mode. In this control mode, when the AC voltage drops at the inverter side, the increase in reactive power absorbed by the inverter compromises the recovery process of the bus voltage; (ii) the constant current (CC) at rectifier and CEA at inverter control mode. In this control mode, when the AC voltage drops at the inverter, the fall in DC transmission power compromises frequency stability [11]; (iii) the CP or CC at rectifier and constant voltage (CV) at inverter control mode. The extinction angle of the inverter decreases when the AC voltage drops. Therefore, the reactive power of the inverter will not increase too much, which could facilitate the voltage stability of the AC/DC joint bus.

Two typical start-up modes are used by HVDC systems, i.e. zero-voltage and zero-current modes. In the zero-voltage mode, the DC current quickly attains its rated value. Initially, the DC voltage increases a little faster and is limited to 0.5 p.u. until the DC current reaches its rated value. Then, the voltage rises gradually to the rated voltage during the slow increase of generator outputs. The zero-voltage mode involves three key issues: (i) the rise in generator output is slower than the rise of HVDC power can be controlled by the converter so that co-operation is essential; (ii) the DC current may overflow during the start; (iii) the converter valve must meet the requirements for zero-power operation. In the zero-current mode, the DC voltage is set to the required value and the DC current increases according to the transmission power required. In this mode, DC current intermittence may develop [13]; this can be avoided by choosing an appropriate, minimum DC current. The start-up mode varies with the converter operation situation. The zero-current start-up mode is employed in this study to ensure voltage stability of the weak power grid.

Therefore, the CC–CV mode is used at starting. During the power lifting, the control mode at rectifier is switched to CP mode. In the zero-current mode, the DC voltage may be the rated voltage or 80 or 70% of that voltage or the voltage of power used to melt ice. During black-starting, the power grid cannot accept a sudden power surge because the grid is weak and the load light.

As the black-start begins, the HVDC system delivers reactive power to the grid when a filter detects a light load in the DC links. As the load increases, the reactive power consumed by the HVDC system will increase with the rise in active power supply; the HVDC system is activated when the voltage attains almost 70% of the rated voltage.

In [11], it was shown that a unipolar voltage of 70% was optimal during black-starting, reducing the impact of DC power on the system, which increases the capacity of the HVDC system to absorb reactive power. As the real minimum continuous current is 5–10% of the rated value, the start current is chosen to be 10% of the rated value to avoid DC intermittence.

2.2 DC power increases during the restoration

When the voltage is stable, a change in HVDC transmission power principally affects the frequency of the system. An imbalance in active power will cause frequency fluctuation, especially in the AC systems that adjust poorly to power loading during black-start. When HVDC system power increases too rapidly or excessively, the frequency of the connected AC system is being compromised. Therefore, in this study, it is considered that the increase in HVDC power should satisfy [11]

$$\Delta P_{\mathrm{dref}} = \frac{2H_{\Sigma}\Delta f}{f_0 \Delta t} \tag{1}$$

where ΔP_{dref} is the increase in DC power, H_{Σ} is the sum of the inertial constants of the generators by reference to the base power S_{B}, Δf is the frequency fluctuation deviation, f_0 is the rated frequency, and Δt is the delay time for a load pickup.

During the restoration, the increased value of the DC power for a certain time is calculated according to the frequency fluctuation.

2.3 DC voltage increases during the restoration

At the beginning of black-start, the reactive power supplied by the input filters is greater than that consumed by the converter. The DC power and DC voltage increase should ensure that no over-voltage phenomenon develops in the converter bus when determining the reference DC voltage control. Therefore, the reference value of the DC voltage controller U_{dref} should satisfy (2) during the black-start [11]

$$S_{\mathrm{ac}}\frac{\Delta U}{U} \geq \left| Q_{\mathrm{f}} - P_{\mathrm{d}} \cdot \sqrt{\frac{U_{\mathrm{d0}}^2}{U_{\mathrm{dref}}^2} - 1} \right| \tag{2}$$

where S_{ac} is the short-circuit capacity of the converter bus; U is the voltage of the converter bus before the connection converter start-up; ΔU is the maximum deviation of the voltage amplitude (here 0.1 p.u); Q_{f} is the reactive power provided by the filter with the required minimum capacity (in general, two sets of double-tuning filters should be used to remove the 12/24 and 3/36 harmonics, respectively); P_{d} is the active power transmitted by the HVDC system; U_{d0} is the ideal no-load DC voltage; and $|\cdot|$ is the absolute value.

2.4 Required power constraints

To ensure system stability during black-start involving an HVDC system, the effective short-circuit ratio (ESCR) needs to be considered. The active and reactive powers of the HVDC system should ensure that ESCR is >2 [14], rendering the system sufficiently strong to weather disturbances, as described in

$$\mathrm{ESCR} = \frac{S_{\mathrm{ac}} - Q_{\mathrm{c}}}{P_{\mathrm{d}}} \tag{3}$$

where Q_{c} is the reactive compensation capacity.

3 Requirements of the AC system considering the HVDC effects

When DC transmission commences at 10% of the rated current and 70% of the rated voltage, there are two requirements of the AC system during black-start: (i) the fundamental voltage magnitude of the steady state should not exceed 1.1 p.u. and (ii) the frequency fluctuation should be between 49 and 51 Hz. To satisfy these requirements, the conditions that must be imposed on the AC system are discussed in the following sections.

3.1 Requirement for short-circuit capacity

As the reactive power provided by the filters at the converter station cannot entirely be consumed by the HVDC system at the start stage that power will be injected into the weak AC power grid, increasing the AC bus voltage. Therefore, to ensure that the voltage does not exceed 1.1 p.u., the short-circuit capacity of the converter bus should satisfy

$$S_{\mathrm{ac}} \geq \frac{U}{\Delta U}(Q_{\mathrm{f}} - Q_{\mathrm{d}}) \tag{4}$$

where Q_{d} is the reactive power consumed by the converter when the HVDC system starts up.

Taking the inverter as an example, the reactive power can be calculated by

$$Q_{\mathrm{d}}^2 = P_{\mathrm{d}}^2\left(\frac{U_{\mathrm{d0}}^2}{U_{\mathrm{d}}^2} - 1\right) \tag{5}$$

$$U_{\mathrm{d}} = U_{\mathrm{d0}}\cos\gamma - \frac{6}{\pi}X_{\mathrm{r}}I_{\mathrm{d}} \tag{6}$$

where U_{d} and I_{d} are the DC voltage and current when the HVDC system starts up, γ is the extinction angle, and X_{r} is the equivalent commutation reactance. For an HVDC transmission system operating at 10% of the rated current and 70% of the rated voltage when starting, $Q_{\mathrm{d}} \simeq 1.05\,P_{\mathrm{d}}$.

3.2 Requirement for effective HVDC inertial constant

When an HVDC system connects to a weak AC system, the large injection of active power causes frequency fluctuations. The system inertia reflects the ability to stabilise frequency. To represent the relationship between system inertia and the active power imparted by the HVDC system, CIGRE defines the effective inertial constant H_{dc} of the HVDC system [10] as

$$H_{\mathrm{dc}} = H_{\Sigma}\frac{S_{\mathrm{G}}}{P_{\mathrm{d}}} \tag{7}$$

where S_G is the total capacity of the corresponding weak AC system and H_Σ is the sum of the inertial constants of generators by reference to the base power S_B, as seen in

$$H_\Sigma = \sum_{i=1}^{n} H_i \frac{S_{Ni}}{S_B} \tag{8}$$

where H_i is the inertial constant of the ith generator and S_{Ni} is the ith generator's capacity.

With respect to the relationship between active power and frequency fluctuation, HVDC demand power and AC system capacity can be obtained by

$$\frac{P_d}{S_G} \le K \frac{\Delta f}{f_N} \tag{9}$$

where K is the comprehensive frequency factor, Δf is the frequency fluctuation deviation, and f_N is the rated frequency.

The effective inertial constant of HVDC system H_{dc} is determined by (7)–(9) combined with the characteristics of the generators in the system.

3.3 Black-starting with LCC–HVDC systems

The requirements of the HVDC and AC systems, their interaction, the start path, and the minimum generator output limit, as well as generator ramping speed, are considered for black-starting with HVDC systems. The process of black-start involving HVDC systems can be described as follows:

(i) The black-start units are the power sources that are initially restored [15]; other generators and the HVDC system are then started.
(ii) Considering the requirements of HVDC and AC system, a priority start-up sequence which indicates the situation when HVDC systems can be injected is developed. A Dijkstra algorithm (which does not use backtracking technology [16]) is used to obtain the transmission paths from power sources to the HVDC system waiting to be started.
(iii) An optimal model for black-start is established by considering the requirements of both the AC and HVDC systems.

4 Calculations for black-start in which LCC–HVDC systems participate

4.1 Priority sequence for LCC–HVDC systems

The shortest recovery path to the AC/DC joint bus and the requirements of HVDC start-up both be considered during priority sequencing. A Dijkstra method [15] is used to define the shortest recovery path (from sources to targets) based on the network topology and branch weight. The shortest power recovery path of the AC/DC joint bus is obtained using the method proposed in [16]. The modelling of HVDC systems in this study is based on the static converter equations and functional effects of the controls in [10].

During the black start-up process, the transmission lines are always light loaded. Hence, the reactive power injected from the shunt branch of the transmission line would lead to overvoltage. Therefore, a high-voltage reactor is always used when starting the line to absorb the extra reactive power to eliminate the overvoltage phenomenon. The total weight of the shortest recovery path of the kth bus is defined as

$$\begin{aligned} W(k) &= \sum W_i \\ W_i &= \max\{mT_i + (Q_{Ci} - Q_{Li}), 0\} \end{aligned} \tag{10}$$

where W_i is the weight of branch i, T_i is the start time weight of branch i, m is a time-to-weight coefficient ensuring that the lines have higher priority than the transformers, Q_{Ci} is the per-unit charging power of branch i, and Q_{Li} is the per-unit high-voltage reactance.

The higher effective inertial constants of HVDC systems indicate that such systems supply more active power to networks with the same S_G values. An AC system with a greater short-circuit capacity can withstand more reactive power from an HVDC system. Therefore, $D(k)$ is defined as a performance measure of the HVDC system to be started, as calculated by

$$D(k) = \frac{H_{dc}(k)}{S_{ac}(k)} \tag{11}$$

Considering the effects of both the shortest recovery path to the AC/DC joint bus and the performance of the HVDC system to be started, the priority sequence of the HVDC system is

$$R_D(k) = W(k) + D(k) \tag{12}$$

The HVDC system with the lowest priority sequence value is preferred for early starting. $W(k)$ and $D(k)$ are linearised and normalised coefficients, respectively. An HVDC system is of higher priority when the priority index R_D is smaller.

4.2 Optimisation of black-starting

After the blackout, the primary task of power system restoration is to start all generators as soon as possible, to restore the full generating capacity of the system while avoiding any subsequent outage. The objective function is obtained by minimising the ramp time of all generators when starting a single generator or an HVDC system [17] in

$$\min f(x) = \max_{l=1}^{m} \left\{ t_l = \left| \frac{P_l - P_0^l}{r_{pl}} \right| \right\} \tag{13}$$

where P_l is the active power of the lth generator, P_0^l is the previous active power of the lth generator, r_{pl} is the ramp rate of the lth generator, and t_l is the adjustment time required by the lth generator. The constraint equations, as shown in (14), pertain principally to power flow and the characteristic constraints on the active and reactive power relationships of the HVDC system

$$\begin{cases} P_{Gi} + P_{di} - P_{Di} - U_i \sum_{j=1}^{j=n} U_j (G_{ij}\cos\theta_{ij} + B_{ij}\sin\theta_{ij}) = 0 \\ Q_{Gi} + Q_{ci} - Q_{Di} - Q_{di} - U_i \sum_{j=1}^{j=n} U_j (G_{ij}\sin\theta_{ij} - B_{ij}\cos\theta_{ij}) = 0 \\ Q_{di}^2 = P_{di}^2 \cdot \left(\frac{U_i^2}{U_d^2} - 1 \right) \end{cases} \tag{14}$$

where i is the bus index, U and θ are the amplitude and phase angle of the bus voltage, P_G and Q_G are the active and reactive powers of the generators, P_d and Q_d are the active and reactive powers of the HVDC system, Q_c is the reactive compensation, P_D and Q_D are the active and reactive loads, and U_d is the DC voltage.

The inequality constraints include bus voltage, the active and reactive powers of the generators, the active and reactive powers of the HVDC system, and the active and reactive loads and the capacity of the reactive compensation equipment. The upper and lower limits of HVDC active and reactive powers are determined by reference to the power recovery requirements discussed in Section 2. The active power constraints on the HVDC system are determined principally by the ESCR of the system studied in Section 3. The reactive power consumed in the HVDC system is affected principally by the voltage fluctuation requirements. The inequality constraints are shown below:

$$\begin{cases} U_{i\min}^2 \le U_i^2 \le U_{i\max}^2 \\ P_{\mathrm{G}i\min} \le P_{\mathrm{G}i} \le P_{\mathrm{G}i\max} \\ P_{\mathrm{D}i\min} \le P_{\mathrm{D}i} \le P_{\mathrm{D}i\max} \\ P_{\mathrm{d}i\min} \le P_{\mathrm{d}i} \le P_{\mathrm{d}i\max} \\ Q_{\mathrm{G}i\min} \le Q_{\mathrm{G}i} \le Q_{\mathrm{G}i\max} \\ Q_{\mathrm{D}i\min} \le Q_{\mathrm{D}i} \le Q_{\mathrm{D}i\max} \\ Q_{\mathrm{d}i\min} \le Q_{\mathrm{d}i} \le Q_{\mathrm{d}i\max} \\ Q_{\mathrm{c}i\min} \le Q_{\mathrm{c}i} \le Q_{\mathrm{c}i\max} \end{cases} \quad (15)$$

where $U_{i\max}$ and $U_{i\min}$ are the upper and lower limits of the ith bus voltage amplitude, respectively; $P_{\mathrm{G}i\max}$ and $P_{\mathrm{G}i\min}$ the upper and lower limits of the active generator power for the ith bus, respectively; $Q_{\mathrm{G}i\max}$ and $Q_{\mathrm{G}i\min}$ are the upper and lower limits of reactive generator power in the ith bus, respectively; $Q_{\mathrm{D}i\max}$ and $Q_{\mathrm{D}i\min}$ are the upper and lower limits of active load power on the ith bus, respectively; $Q_{\mathrm{d}i\max}$ and $Q_{\mathrm{d}i\min}$ are the upper and lower limits of reactive DC system power for the ith bus, respectively; and $Q_{\mathrm{c}i\max}$ and $Q_{\mathrm{c}i\min}$ are the upper and lower limits of the reactive compensation capacity of the ith bus, respectively

$$\begin{aligned} P_{\mathrm{d}i\min} &= 0.1 P_{\mathrm{dN}i} \\ P_{\mathrm{d}i\max} &= \frac{S_{\mathrm{ac},i} - Q_{\mathrm{c}i\min}}{\mathrm{ESCR}_{\min}} \end{aligned} \quad (16)$$

$$\begin{aligned} Q_{\mathrm{d}i\max} &= 10 S_{\mathrm{ac},i} + Q_{\mathrm{c}i\max} \\ Q_{\mathrm{d}i\min} &= Q_{\mathrm{c}i\max} - 10 S_{\mathrm{ac},i} \end{aligned} \quad (17)$$

The non-linear interior-point method [18, 19] is used to solve the optimisation model. If, within the ranges of the inequality constraints, no power flow solution is possible, the optimal power flow (OPF) will diverge because of the mismatch between the equality and inequality constraints, regardless of the type of OPF used [16]. When the OPF diverges, the next HVDC in the start-up sequence will attempt to start. If no HVDC in the start-up sequence has been successfully started, an effort will be made to start the highest-priority generator. The flow chart for black-start recovery optimisation involving HVDC systems is shown in Fig. 1.

In addition, the minimum HVDC power in China is 10% of the rated power. Hence, the active power of the HVDC system should increase to 0.1 p.u. as soon as possible after starting.

5 Examples and results

5.1 Test system

Regions of the Guangdong power grid, including the Guangzhou and Dongguan grids with multi-infeed HVDC systems, are used to verify our restoration strategy. There are 192 buses, 39 generators, 315 power transmission lines, and 3 HVDC-receiving ends. The brief construction of the test system is shown in Fig. 2, where the diagrams are labelled.

The black-start generators are located in the Hengyun D plant having a capacity of 2 × 330 MW; the ramp rate is 2.4 and cos φ = 0.914. During black-start, one generator in that plant is chosen to provide the active and reactive powers of 18 MW and 8 MVar, respectively.

It should be mentioned that the test system is also built in PSD-BPA, which is an electromechanical transient simulation software developed by China EPRI. Each step is verified in PSD-BPA, and the results show that the control characteristics of LCC–HVDC systems can reach the steady-state operation point calculated by the proposed algorithm.

5.2 Black-start without LCC–HVDC system participation

The calculated recovery sequence on black-start without an HVDC system [16] is shown in Fig. 3.

In Fig. 3, the circular blocks represent areas with generators and the other blocks represent areas without generators. The number on the arrow lines represent the start sequence and direction. The restoration started from the power station named ‘HEY’, and then the LUNTOU substation is started, then ZENGCHEN station, and so on.

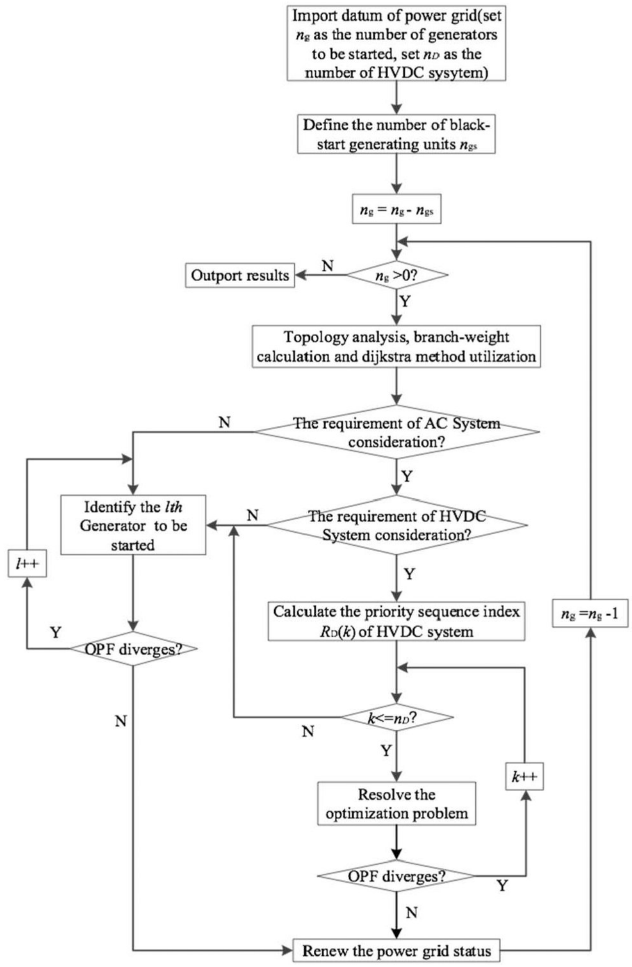

Fig. 1 *Flow chart for black-starting using LCC–HVDC systems*

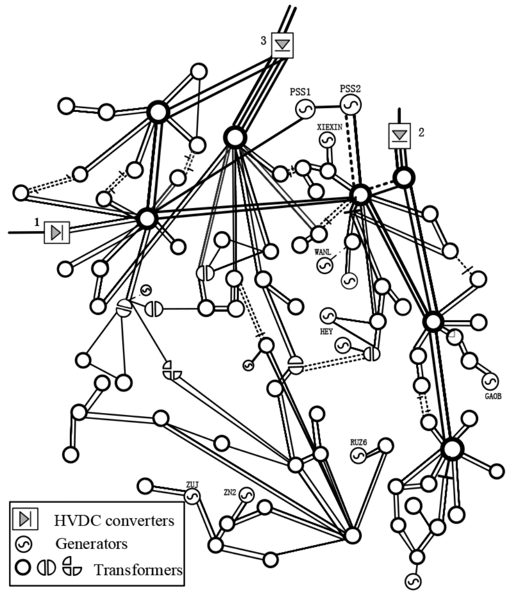

Fig. 2 *Brief construction of the test system*

5.3 Black-start with HVDC system participation

When the system satisfies the requirements for HVDC start-up, the proposed methods are utilised. The model of HVDC systems provided in [10] is utilised here. The power order and current order

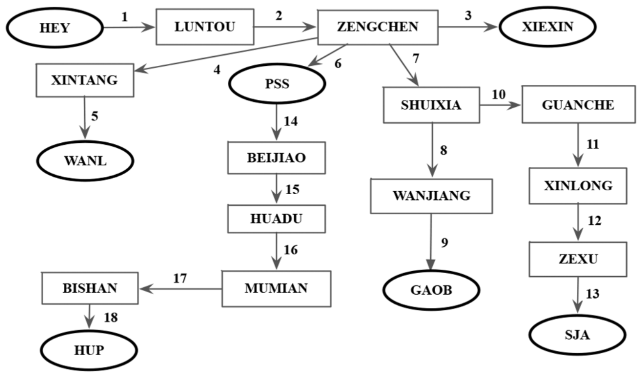

Fig. 3 *Black-start sequence without an HVDC system*

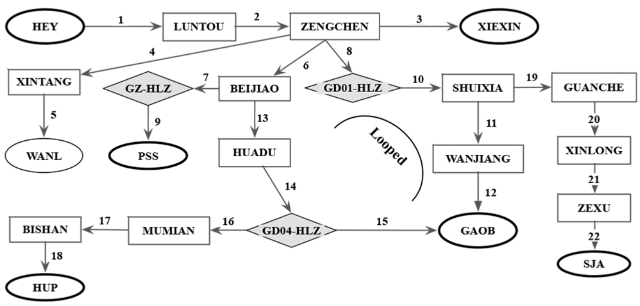

Fig. 4 *Black-start sequence involving HVDC systems*

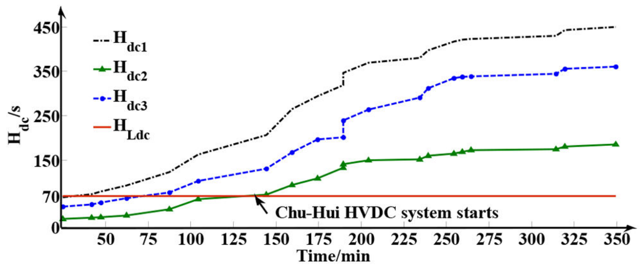

Fig. 5 *Change in the effective inertial constants of each HVDC system*

are determined in (1) and (2). The reference of ignition delay angle and extinction angle are set as 15° and 18°, respectively. Also, the reference of power is set as 100 MVA. The first HVDC line is started with 10% of the rated current and 70% of the rated voltage after seven generators (of indices 13–19) are started. With the increase in load, the second HVDC system starts. After this, generators labelled 22, 24, 25, 26, 27, and 28 get started, followed by the third HVDC system. The optimised recovery sequence is shown in Fig. 4.

In Fig. 4, the circular blocks represent areas with generators, the diamond-shaped blocks represent HVDC converter stations and the other blocks areas without power sources.

The start sequence given by the proposed method is shown in Fig. 4 as seen by the direction and index of the arrow lines. The first HVDC system to join is the Tian-Guang HVDC system in areas GZ–HLZ, which starts at the seventh step after BEIJIAO substation started. The second HVDC system is the Chu-Hui system located in areas GZ01–HLZ, which starts at the eighth step. The third HVDC system is the Niu-Cong system in areas GD04–HLZ at the 14th step after HUADU substation started.

During the restoration, the change in the effective inertial constants of each HVDC system is shown in Fig. 5, where $H_{\rm Ldc}$ is the required minimum inertial constant when starting an HVDC system as calculated by (7)–(9), with $K = 3$ for the China Southern Power Grid, as determined by practical experience [20]. $H_{\rm dc1}$, $H_{\rm dc2}$, and $H_{\rm dc3}$are the $H_{\rm dc}$ values of HVDC systems 1–3.

The variation in the short-circuit capacities of each HVDC system during restoration is shown in Fig. 6, where $S_{\rm Lac1}$, $S_{\rm Lac2}$, and $S_{\rm Lac3}$ represent the lowest limits of $S_{\rm ac1}$, $S_{\rm ac2}$, and $S_{\rm ac3}$,

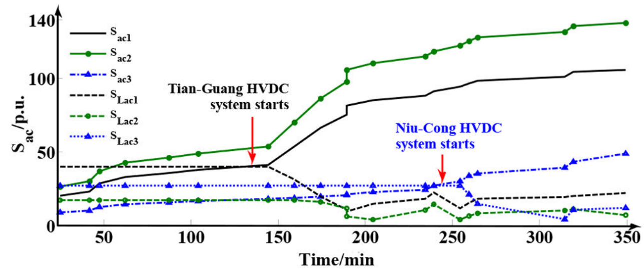

Fig. 6 *Variation in the short-circuit capacities of each HVDC system*

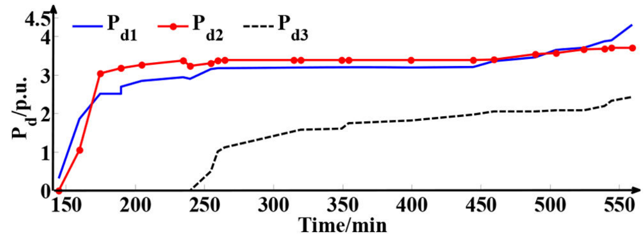

Fig. 7 *Changes in the active power of the three HVDC systems*

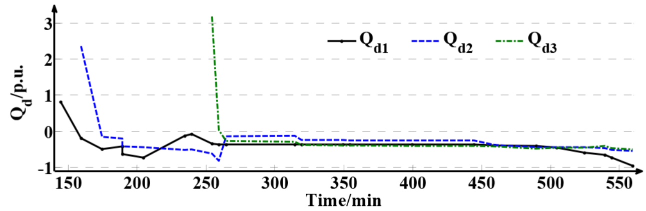

Fig. 8 *Variations in the reactive power of the three HVDC systems*

respectively, for starting the corresponding HVDC systems, as calculated by (4). The system power reference is set as 100 MVA.

As can be observed from Figs. 5 and 6, the key constraints for deciding where to insert the Tian-Guang and Niu-Cong HVDC systems are their short-circuit capacities while the key constraint for deciding where to insert the Chu-Hui HVDC system is the effective inertial constant. When $S_{\rm ac1} = S_{\rm Lac1}$, the Tian-Guang HVDC system starts and when $S_{\rm ac3} = S_{\rm Lac3}$, the Niu-Cong HVDC system starts. When $H_{\rm dc2} = H_{\rm Ldc}$, the Chu-Hui HVDC system starts.

It should be noted that the output power of an HVDC system cannot reach the rated value during black-start. In order to achieve minimum starting DC power and provide the necessary power for the AC/DC system, the active power of the three HVDC systems increases fast in the beginning under the zero-current stat-up mode and the CC–CV control mode. Then the active power plateaus in the rest of the restoration proceed as some main generators have been started. That is also related to the stability of the power system. The changes in the active power of the three HVDC systems are shown in Fig. 7.

The variations in the reactive power of the three HVDC systems are shown in Fig. 8. When an HVDC system starts, the reactive power is positive in the beginning because the filter is on. As the DC load increases, the reactive power consumed by the HVDC system also increases, thus the output reactive power decreases to negative. According to the proposed start-up and recovery method, the reactive compensations are inserted to increase the stability of the system when the converter absorbs reactive power.

5.4 Comparison of the two black-start processes

The total ramp time indicates the speed of power system restoration. Shorter time means better for the restoration. The total ramp time for each generator as the start power source is shown in Fig. 9. The *x*-axis represents the index of the generator. With the HVDC systems participating in, the total ramp time of most generators decreases; thus, the start-up is accelerated and restoration time is reduced.

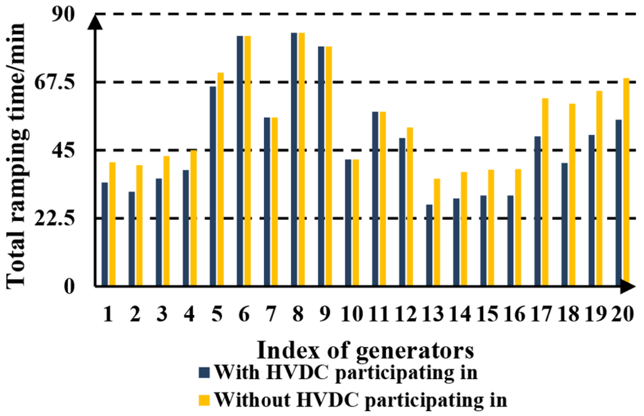

Fig. 9 *Total ramp time of each generator during the two black-start processes*

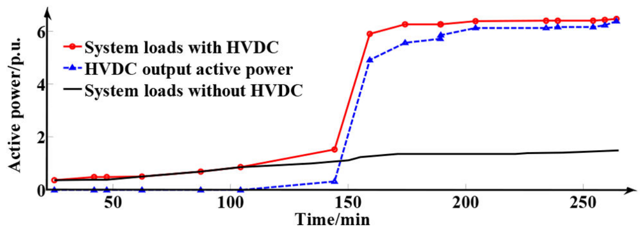

Fig. 10 *Active loads of the two black-start processes and the contribution of HVDC power*

Furthermore, the pick-up load of the power system is also an indicator of the power system recovery effect. The active power loads of the two black-start processes, and the contributions of HVDC power are shown in Fig. 10. The curves show that the load is improved by the HVDC systems.

6 Conclusion

The method for AC/DC system black-start and recovery using LCC–HVDC systems is presented in this study. It is proved that HVDC systems can be used in specific situations. The main contributions of this work are as follows:

(i) It is observed that when HVDC systems engage themselves in black-start by analysing the start-up mode, the DC power and voltage increases, and power constraints.
(ii) The short-circuit capacity of the AC system, the effective inertial constant of the HVDC system, and AC system conditions in terms of HVDC black-starting are explored.
(iii) During black-start, a priority sequence is developed, which indicates the situation when HVDC systems should be started. The calculations for requirements of the HVDC system's insertion are performed, and both the HVDC system start-up and recovery are analysed.

The proposed method enables LCC–HVDC systems to join in black-start when various constraints are met. Compared to conventional black-start, insertion of LCC–HVDC systems stabilises the grid, shortens the recovery time, and reduces the economic and social losses caused by large blackouts. However, the details of load pick-up, transformer charging times, and the response times of reactive compensation and the circuit breakers are not considered in this study.

7 Acknowledgments

This work was supported by the Science and Technology Foundation of Guangdong Power Grid Corp. Ltd (GDKJXM00000030).

8 References

[1] Galias, Z.: 'Probabilistic model for studying blackouts in power networks', *IEEE J. Emerg. Sel. Top. Circuits Syst.*, 2017, **PP**, (99), pp. 1–10

[2] Australian Energy Market Operator: 'Preliminary report—black system event in South Australia on 28 September 2016', 2016, pp. 1–20

[3] Rampurkar, V., Pentayya, P., Mangalvedekar, H.A., *et al.*: 'Cascading failure analysis for Indian power grid', *IEEE Trans. Smart Grid*, 2016, **7**, (4), pp. 1951–1960

[4] Veloza, O.P., Santamaria, F.: 'Analysis of major blackouts from 2003 to 2015: classification of incidents and review of main causes', *Electr. J.*, 2016, **29**, (7), pp. 42–49

[5] Hogan, W.W.: 'Discussion on 'optimal generator start-up strategy for bulk power system restoration'', *IEEE Trans. Power Syst.*, 2012, **19**, (1), p. 690

[6] Lindstrom, R.R.: 'Simulation and field tests of the black start of a large coal-fired generating station utilizing small remote hydro generation', *IEEE Trans. Power Syst.*, 1990, **5**, (1), pp. 162–168

[7] Wei, S., Liu, C.C., Zhang, L.: 'Optimal generator start-up strategy for bulk power system restoration', *IEEE Trans. Power Syst.*, 2011, **26**, (3), pp. 1357–1366

[8] Gu, X., Zhong, H.: 'Optimization of network reconfiguration based on a two-layer unit-restarting framework for power system restoration', *IET Gener. Transm. Distrib.*, 2012, **6**, (7), pp. 693–700

[9] Zhang, C., Lin, Z., Wen, F., *et al.*: 'Two-stage power network reconfiguration strategy considering node importance and restored generation capacity', *IET Gener. Transm. Distrib.*, 2014, **8**, (1), pp. 91–103

[10] Kundur, P.: '*Power system stability and control*' (McGraw-Hill Inc., New York, 1994, 1st edn.)

[11] Xu, G., Tu, L., Lan, H., *et al.*: 'Analysis on HVDC start-up in system black-start'. Int. Conf. on Electric Utility Deregulation and Restructuring and Power Technologies, Changsha, China, 2016, pp. 1705–1709

[12] Li, B., Liu, T., Xu, W., *et al.*: 'Research on technical requirements of line-commutated converter-based high-voltage direct current participating in receiving end AC system's black start', *IET Gener. Transm. Distrib.*, 2016, **10**, (9), pp. 2071–2078

[13] Wang, H.-W., Zeng, N.-C., Jiang, W.-P., *et al.*: 'Study on minimal startup power of ±660 kV HVDC power transmission system under islanded operation at sending system', *Power Syst. Technol.*, 2010, **34**, (5), pp. 83–87

[14] Xin, H., Zhang, F., Yu, Y., *et al.*: 'Generalized short circuit ratio for multi-infeed DC systems: definition and theoretical analysis', *Proc. CSEE*, 2016, **36**, (3), pp. 633–647

[15] Hou, Y., Liu, C.-C., Sun, K., *et al.*: 'Computation of milestones for decision support during system restoration', *IEEE Trans. Power Syst.*, 2011, **26**, (3), pp. 1399–1409

[16] Liu, C., Wu, M., Deng, Y.: 'Start-up sequence of generators in power system restoration avoiding the backtracking algorithm'. 2013 IEEE Power & Energy Society General Meeting, Vancouver, Canada, 2013, pp. 1–5

[17] Liu, C., Wu, M., Xu, W., *et al.*: 'Optimisations model for online generators when a new generator is about to get started during power system restoration process', *IET Gener. Transm. Distrib.*, 2017, **11**, (1), pp. 57–63

[18] Tate, J.E., Overbye, T.J.: 'A comparison of the optimal multiplier in polar and rectangular coordinates', *IEEE Trans. Power Syst.*, 2005, **20**, (4), pp. 1667–1674

[19] Imene, T., Djamel, B., Adnan, Y.: 'A feasible primal-dual interior point method for linear semidefinite programming', *IEEE Trans. Signal Process.*, 2016, **312**, pp. 216–230

[20] Zhou, J., Li, J.S., Su, Y.S.: 'Analysis on start-up conditions of HVDC system in black-start', *Autom. Electr. Power Syst.*, 2011, **35**, (3), pp. 92–96